0273-2289/03/105-108/0593/$20.00

Flow Field in a Shrinking-Bed Reactor for Pretreatment of Cellulosic Biomass

Yinkun Wan and Thomas R. Hanley*

Department of Chemical Engineering,
University of Louisville, Louisville, KY 40292,
E-mail: tom.hanley@louisville.edu

Abstract

A shrinking-bed reactor was designed by the National Renewable Energy Laboratory to maintain a constant bulk packing density of cellulosic biomass. The high solid-to-liquid ratio in the pretreatment process allows a high sugar yield and avoids the need to flush large volumes of solution through the reactor. The shrinking-bed reactor is a promising pretreatment reactor with the potential for scale-up for commercial applications. To scale up the shrinking-bed reactor, it is necessary to understand the flow pattern in the reactor. In this study, flow field is simulated with computational fluid dynamics using a porous medium model. Different discrete "snapshots" and multiple steady states are utilized. The bulk flow pattern, velocity distribution, and pressure drop are determined from the simulation and can be used to guide reactor design and scale-up.

Index Entries: Shrinking-bed reactor; computational fluid dynamics; flow field; cellulosic biomass; hydrolysis.

Introduction

Decades ago, the National Renewable Energy Laboratory (NREL) investigated the possibility of producing high yields of glucose from cellulose by thermochemical methods. Complications arose owing to the use of strong acid and high temperatures. Strong acids require significant alkali neutralization. High temperature requires a short residence time to prevent glucose degradation into toxic chemicals. High acid solution flow rates produce large volumes of acid solution that require treatment and heating. Recently, NREL investigated a two-stage, two-temperature dilute-acid pretreatment process *(1–3)*. In the first stage, the temperature is relatively low and much of the hemicellulose hydrolyzes. In the second stage, the temperature rises, hydrolyzing more of the hemicellulose. The

*Author to whom all correspondence and reprint requests should be addressed.

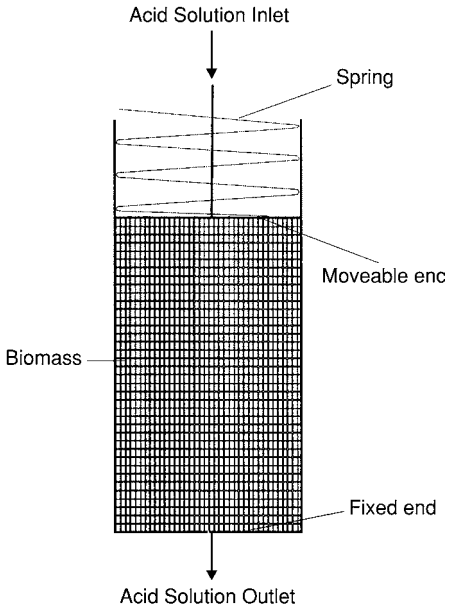

Fig. 1. Structure of shrinking-bed reactor.

countercurrent process shortens the residence time, and two-temperature processing avoids exposure to high temperatures, reducing the degradation and reopening of thermochemical hydrolysis of cellulose. To reduce the acid solution volume and keep high solid-to-liquid ratio, NREL designed a shrinking-bed reactor *(4)*.

The shrinking-bed reactor was designed to keep a constant bulk packing density of solid biomass in the reactor, resulting in a high sugar concentration owing to the high solid-to-liquid ratio, as well as a reduced liquid volume. Figure 1 shows the structure of a laboratory-scale shrinking-bed reactor. This reactor has one fixed end and one movable end. The movable end is supported by a compressed spring. When the reaction processes, the easily processed hemicellulose is hydrolyzed and removed from the packed bed, decreasing the bulk packing-bed density. When the spring-loaded movable end compresses the remaining biomass particles, the bulk packing density remains constant.

Chen et al. *(5)* developed a kinetic model to describe the shrinking-bed reactor and found that shrinking-bed operation increases the sugar yield by about 5% compared with non-shrinking-bed operation. Lee et al. *(6)* also developed a mathematical model to simulate a countercurrent shrinking-bed reactor and show that bed shrinking positively affects both hemicellulose and cellulose hydrolysis. Converse *(7)* presents a model to simulate a cross-flow shrinking-bed reactor for the hydrolysis of lignocellulosics and finds a trade-off between cross-flow and plug-flow shrinking-bed reactors. Cross flow allows higher yields than plug flow but generally with a slight reduction in product concentration.

Previous studies have shown the great potential of the shrinking-bed reactor for commercial application. To scale up the shrinking-bed reactor, the first step is to understand the flow field in a laboratory-scale shrinking-bed reactor. In the present work, computational fluid dynamics (CFD) is used to study flow behavior in a laboratory-scale shrinking-bed reactor.

Model and Method

Porous Media Model

The porous media model *(8)* is used to simulate flows through shrinking-bed operation, (i.e., packed-bed) in which biomass is taken as porous media.

In the porous media model, a momentum source term S_i is added to the standard fluid flow equation.

$$S_i = \sum_{j=1}^{3} D_{ij}\,\mu V_j + \sum_{j=1}^{3} C_{ij}\,\frac{1}{2}\,\rho\,|V_j|\,V_j \tag{1}$$

The first part of Eq. 1 is a viscous loss term and the second is an inertial loss term. For simple homogeneous porous media, S_i can be written as

$$S_i = \frac{\mu}{\alpha}\,V_i + C_2\,\frac{1}{2}\,\rho\,|V_i|\,V_i \tag{2}$$

in which α is the permeability and C_2 is the inertial resistance factor.

In laminar flows through porous media, the pressure is proportional to velocity and C_2 can be taken as zero. Ignoring convective acceleration and diffusion, the porous media model can be changed into Darcy's Law:

$$\nabla P = \frac{\mu}{\alpha}\,V \tag{3}$$

in which ∇P is the pressure drop.

For turbulent flows and for cases in which the permeability term can be eliminated, the porous media model can be rewritten as follows:

$$\frac{\partial P}{\partial x_i} = \sum_{j=1}^{3} C_{2ij}\left(\frac{1}{2}\,\rho V_j\,|V_i|\right) \tag{4}$$

For packed-bed and turbulent flows, Darcy's law can be rewritten as Ergun equation *(9)*:

$$\nabla P = \frac{150\mu}{D_p^2}\,\frac{(1-\varepsilon)^2}{\varepsilon^3}\,V + \frac{1.75\rho}{D_p}\,\frac{(1-\varepsilon)}{\varepsilon^3}\,V\,V \tag{5}$$

For laminar flow, the second term of the Ergun equation may be dropped, resulting in the Blake-Kozeny equation:

$$\nabla P = \frac{150\mu}{D_p^2}\,\frac{(1-\varepsilon)^2}{\varepsilon^3}\,V \tag{6}$$

Table 1
Different Simulated Stages

Status	Packed-bed height (m)	Packed-bed diameter (m)	Inlet port diameter (m)	Outlet port diameter (m)	Flow rate (m^3/s)	Grid ($X \times Y$)
Initial (100%)	0.160	0.040	0.008	0.008	1.256×10^{-7}	20×53
80% of initial height	0.128	0.040	0.008	0.008	1.256×10^{-7}	20×43
60% of initial height	0.096	0.040	0.008	0.008	1.256×10^{-7}	20×32
40% of initial height	0.064	0.040	0.008	0.008	1.256×10^{-7}	20×32
20% of initial height	0.032	0.040	0.008	0.008	1.256×10^{-7}	20×32

Comparing Eqs. 3 and 4 with Eq. 5,

$$\alpha = \frac{D_p^2}{150} \frac{\varepsilon}{(1-\varepsilon)^2} \tag{7}$$

$$C_2 = \frac{3.5}{D_p} \frac{(1-\varepsilon)}{\varepsilon^2} \tag{8}$$

in which D_p is the mean particle diameter, and ε is the void volume fraction of the packed bed.

Experimental Method

The commercial CFD package FLUENT 5.5 was used to simulate a laboratory-scale shrinking-bed reactor. Since the shrinking process cannot be simulated in Fluent 5.5, we took several discrete "snapshots" to simulate the shrinking process assuming the biomass particle diameter and void fraction remain constant.

The shrinking-bed reactor's operation conditions were as follows:

Flowing media: water (liquid); temperature: 298K; heat transfer: none; flow regime: laminar; inlet velocity: 2.5×10^{-3} m/s; outlet pressure: 1 atm; particle diameter (D_p): 1 mm; packed-bed void fraction (ε): 0.2; $(1/\alpha) = 1.72 \times 10^{11}$; and $C_2 = 3.5 \times 10^5$.

Initial and subsequent snapshot states are given in Table 1.

Results and Discussion

Flow Pattern by Velocity Vector

The velocity vectors in 100, 80, 60, 40, and 20% initial bed height are shown in Fig. 2. The flow in the shrinking-bed reactor is mainly plug flow except for some radial flow in the bed corners. As the bed shrinks, the percentage of plug flow volume in the whole bed decreases. Since plug flow is a positive factor in the mass transfer process, the mass transfer efficiency will decrease as the bed shrinks.

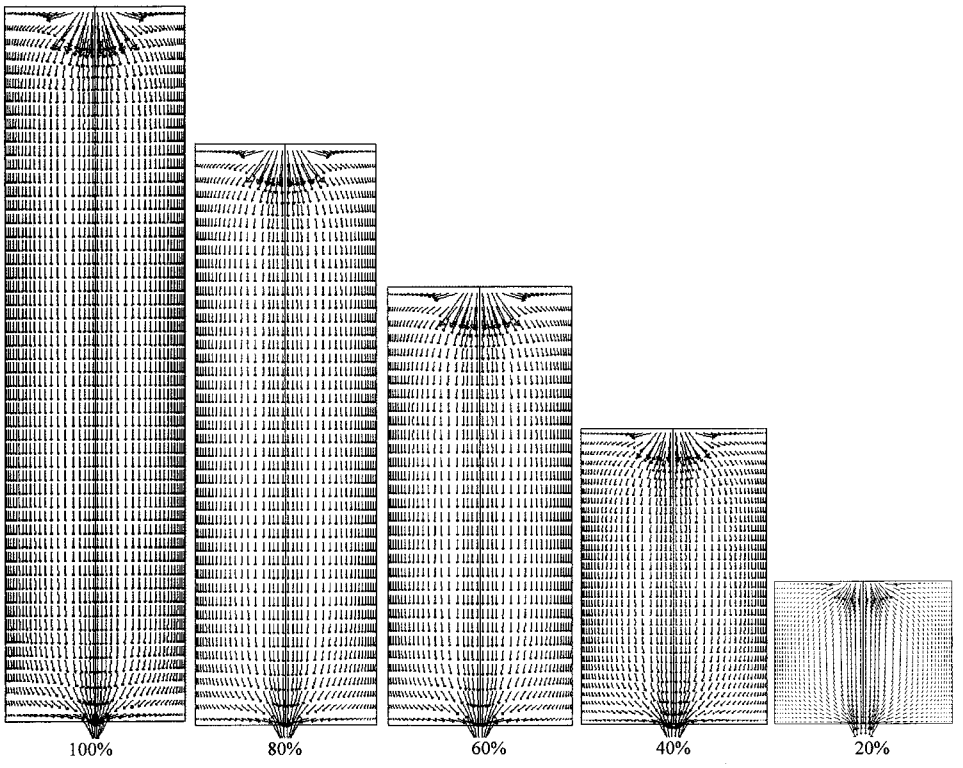

Fig. 2. Flow patterns in the shrinking-bed reactor.

To keep plug flow in the entire shrinking bed, one option is to create even fluid distribution in the inlet and outlet. Figure 3 shows the flow pattern of the shrinking-bed reactor with the inlet acid solution evenly distributed over the bed diameter. Apparently, this change reduces radial flow in the top corner and improves the mass transfer efficiency. If the outlet flow could also be evenly distributed, the radial flow in the bottom corner would disappear, enhancing the shrinking-bed reactor's performance.

Axial and Radial Velocity Distributions

In this simulation, the *X* direction is radial, with positive *X* velocity toward the reactor wall; *Y* is for axial direction, with positive *Y* velocity indicating upward flow.

X velocity distributions for 80% initial bed height are shown in Fig. 4. Clearly, radial flow exists in the corners of the shrinking bed. The radial flow can increase the residence time and has different impacts on production of sugars. If the hydrolysis process is controlled by chemical kinetics and has not reached equilibrium, then an increase in residence time can enhance production of sugars; if the hydrolysis has reached equilibrium, the increase in residence time will result in sugar degradation.

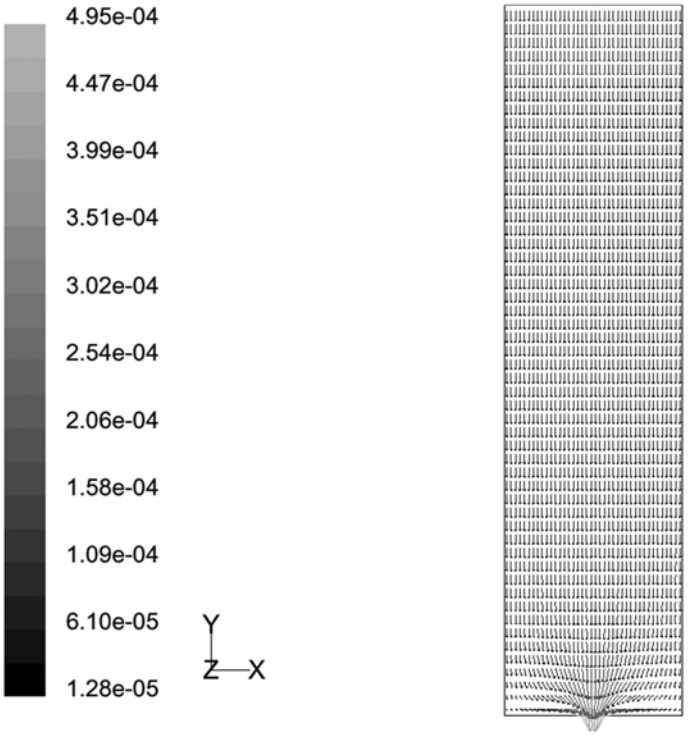

Fig. 3. Flow pattern and fluid velocities in meters per second in the shrinking-bed reactor with optimized inlet.

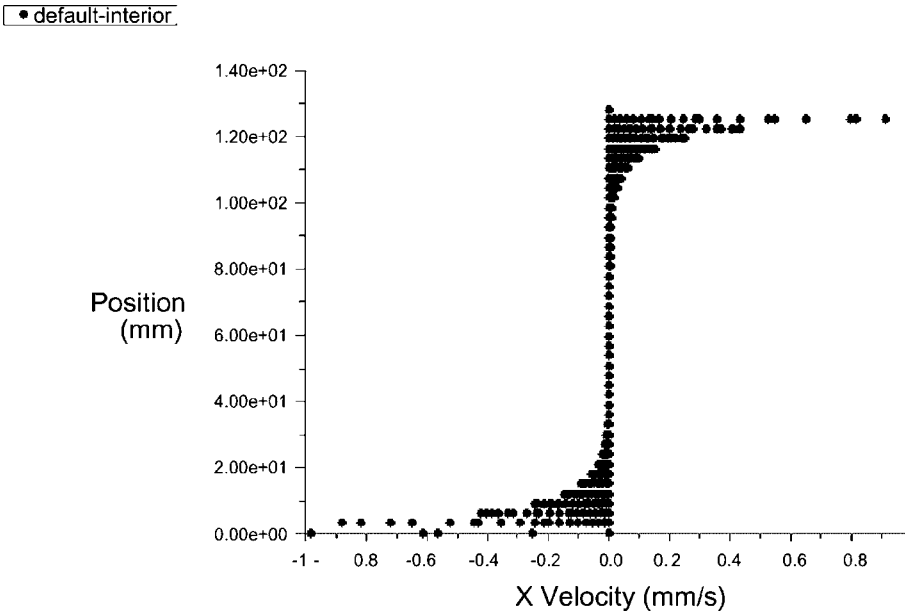

Fig. 4. Radial velocity distribution at 80% bed height.

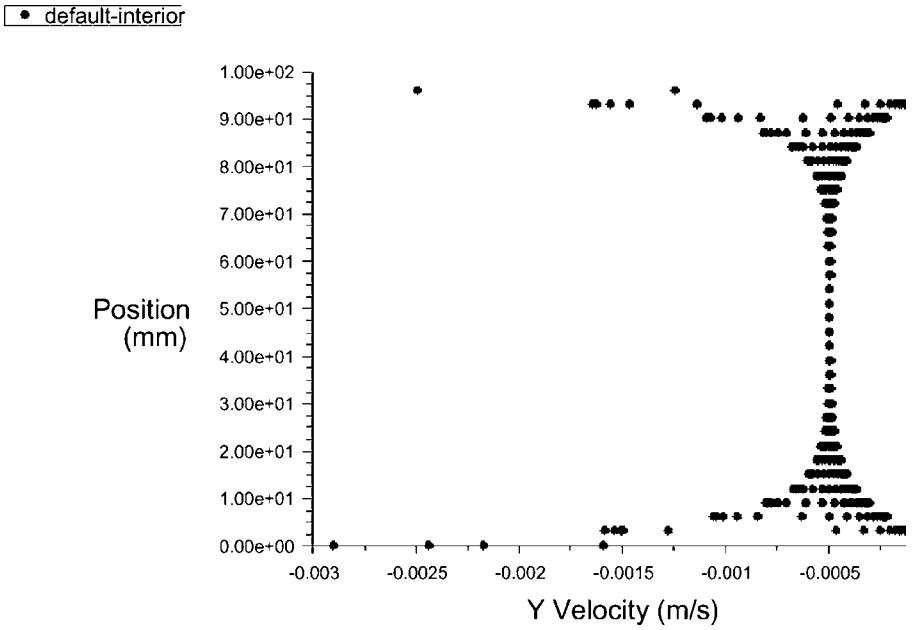

Fig. 5. Axial velocity distribution at 60% bed height.

Results from the *Y* velocity distributions along the axis in 100, 80, 60, 40, and 20% initial bed height show a uniform *Y* velocity distribution, or plug flow, in the middle of the bed. The uniform *Y* velocity area decreases rapidly from about 60 to 0% in the whole bed volume when the bed height shrinks from 100 to 20%. Moreover, it is observed that with no positive *Y* velocity, no backflow occurs in the shrinking-bed reactor. Thus, the shrinking-bed reactor is ideal for mass transfer and, as a result, can stimulate the hydrolysis reaction. In this aspect, the shrinking-bed reactor is suitable for bioethanol production. Typical *Y* velocity distribution along the axis is shown in Fig. 5.

Pressure Drop

Typical pressure distribution contours in the shrinking-bed reactor are shown in Fig. 6, where it is indicated that the pressure distribution is not even. The highest static pressure occurs in the fluid inlet while the lowest pressure appears in the fluid outlet. The higher pressure in the upper bed level may result in higher hydrolysis reaction rates in this area.

In Fig. 7, pressure distributions for different bed heights are plotted in the central axis (symmetry line). As the bed shrinks, the pressure drop decreases. As the bed height decreases from 100 to 20% of initial height, the pressure drop decreases from 1.7×10^4 to 5.8×10^3 Pa. The decreased pressure drop has a positive effect on biomass hydrolysis. Initially, a large pressure drop produces greater fluid flow and counters the effect of larger

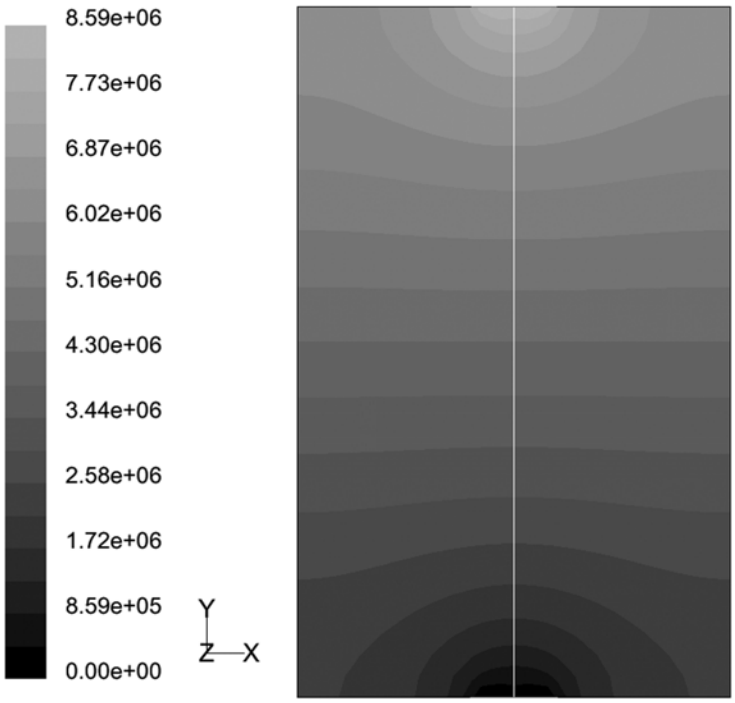

Fig. 6. Static pressure contour (Pa) at 40% bed height.

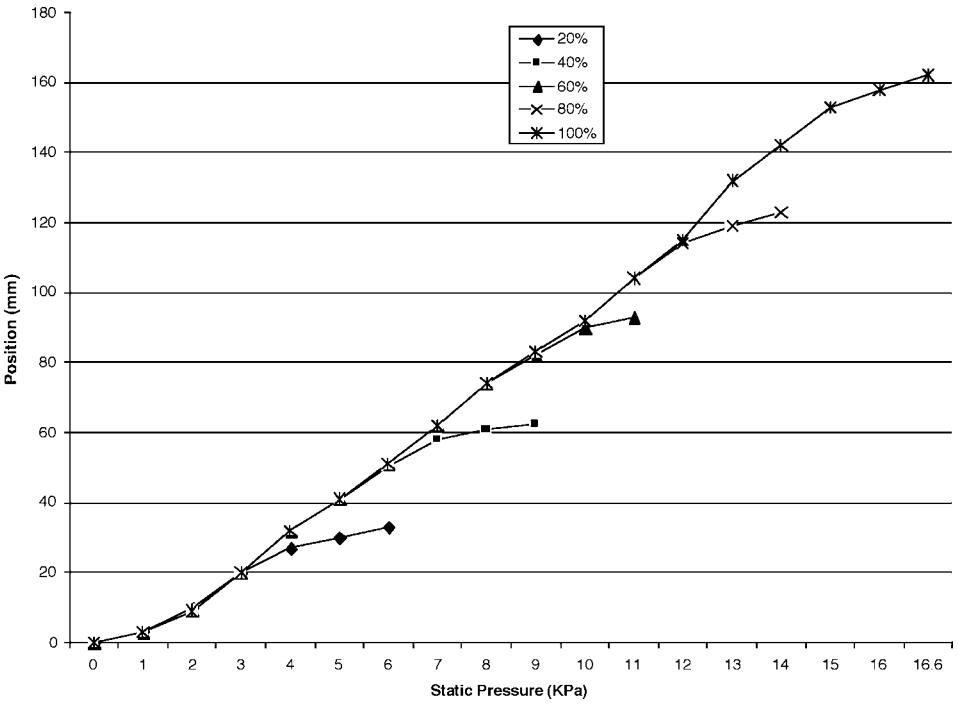

Fig. 7. Pressure distribution along the central axis.

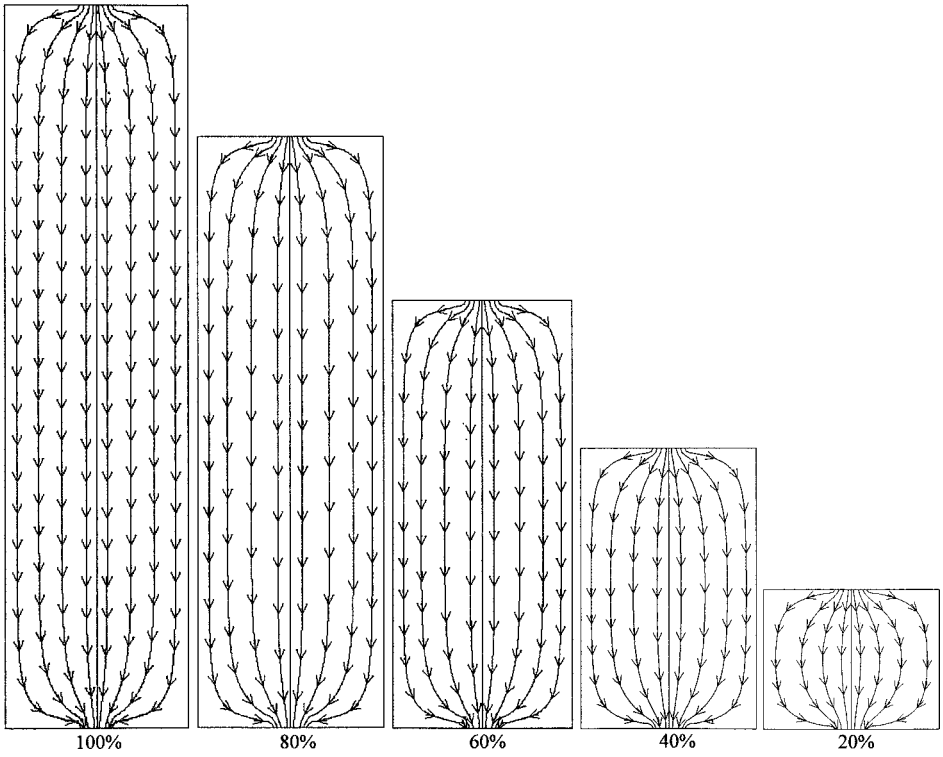

Fig. 8. Path lines in shrinking-bed reactor at five bed heights.

bed height. Increased residence time of fluid in the bed means higher risk of decomposition of sugars into toxic chemicals. In the latter stages, the smaller pressure drop increases residence time and allows more lignocellulose to be hydrolyzed.

Flow Path

Pathlines are used to visualize the flow of massless particles in the problem domain. The particles are released from one or more defined surfaces. In the present work, 10 massless particles were released from the fluid inlet. Figure 8 shows the path lines of the shrinking-bed reactor at different heights and confirms the flow pattern described in Fig. 2.

Conclusions

The CFD simulation for a laboratory-scale shrinking-bed reactor indicated mostly plug flow with some radial flow in the bed corners. No backflow was found. As the bed shrank, the pressure drop of the bed decreased. One suggestion to optimize the flow in this reactor is to adjust the fluid inlet and outlet to produce more even flow distribution. Com-

pared with the non-shrinking-bed reactor, simulation results of the shrinking-bed reactor show that the shrinking process can reduce the residence time of the fluid in the bed as well as the risk of decomposition of sugars into harmful chemicals. Moreover, the bed shrinkage reduces the fluid flow and enhances sugar concentration in the hydrolysate to improve process economics. Therefore, the shrinking-bed reactor is an ideal reactor for bioethanol production.

Nomenclature

C, C_2, D = matrix
D_p = particle diameter (m)
P = pressure (Pa)
S_i = source term for ith momentum equation
V_j = velocity of i direction
α = permeability
ε = void fraction
μ = molecular viscosity (kg/m·s)
ρ = density (kg/m^3)

Acknowledgments

This research was supported by NREL (contract no. XCO-1-31016-01).

References

1. Tucker, M. P., Farmer, J. D., Keller, F. A., Schell, D. J., and Nguyen, Q. A. (1998), *Appl. Biochem. Biotechnol.* **70–72,** 25–35.
2. Nguyen, Q. A., Tucker, M. P., Keller, F. A., Beaty, D. A., Connors, K. M., and Eddy, F. P. (1999), *Appl. Biochem. Biotechnol.* **77–79,** 133–142.
3. Nguyen, Q. A., Tucker, M. P., Keller, F. A., and Eddy, F. P. (2000), *Appl. Biochem. Biotechnol.* **84–86,** 561–576.
4. Torget, R. W., Hayward, T. K., and Elander, R. (1997), presented at the *19th Symposium on Biotechnology for Fuel and Chemicals*, Colorado Springs, CO.
5. Chen, R., Wu, Z., and Lee, Y. Y. (1998), *Appl. Biochem. Biotechnol.* **70–72,** 37–49.
6. Lee, Y. Y., Wu, Z., and Torget, R. W. (2000), *Bioresour. Technol.* **71,** 29–39.
7. Converse, A. O. (2002), *Bioresour. Technol.* **81,** 109–116.
8. Fluent, Inc. (1998) FLUENT 5 User's Guide, vol. 1., Fluent, Inc., Lebanon, NH.
9. Ergun, S. (1952), *Chem. Eng. Prog.* **48(2),** 89–94.